[5]Kuwahara, K., "Study of Flow Past a Circular Cylinder by an Inviscid Model," *Journal of Physical Society of Japan,* Vol. 45, Jan. 1978, pp. 292–297.

[6]Kimura, T. and Tsutahara, M., "Flow Past a Rotating Circular Cylinder at High Reynolds Number," *Journal of Japapese Society of Aeronautical Space Sciences,* Vol. 34, April 1986, pp. 14–20.

[7]Ericsson, L. E., "Karman Vortex Shedding and the Effect of Body Motion," *AIAA Journal,* Vol. 18, Aug. 1980, pp. 935–944.

[8]Matsui, T., "Separation in a Flow past a Circular Cylinder," *Journal of Japanese Society of Aeronautical Space Sciences,* Vol. 20, Nov. 1972, pp. 18–26 (in Japanese).

[9]Freymuth, P., Bank, W., and Palmer, M., "Use of Titanium Tetrachloride for Visualization of Accelerating Flow around Airfoils," International Symposium on Flow Visualization, Ann Arbor, MI, 1983.

[10]Roshko, A., "Experiments on the Flow Past a Circular Cylinder at Very High Reynolds Number," *Journal of Fluid Mechanics,* Vol. 10, 1961, pp. 345–356.

[11]Diaz, F., Gavalda, J., Kawall, J. G., and Keffer, J. F., "Asymmetrical Wake Generated by a Spinning Circular Cylinder," *AIAA Journal,* Vol. 23, Jan. 1985, pp. 49–54.

Numerical Solutions of Viscous Transonic Flow in Turbomachinery Cascades

V. Iyer* and E. von Lavante†
Texas A&M University, College Station, Texas

Introduction

A MODIFICATION to the implicit, block-bidiagonal algorithm for solving the compressible Navier-Stokes equations is presented. The resulting method showed enhanced robustness and computational efficiency; its solution procedure requires only inversions of scalar bidiagonal matrices. In its application to several internal flow configurations, the resulting computational advantage and the importance of viscous effects in transonic cascade flow are presented.

Solution Procedure

Many of the recent studies[1-4] of cascade flow predominantly deal with the inviscid Euler equations; only isolated solution's of the full Navier-Stokes equations are presented. However, in high-solidity blade rows, there is a strong passage shock interacting with the boundary layer. The inviscid model is inadequate in such cases. The solution of the full Navier-Stokes equations is beset with difficulties in that the proximity of the shock-boundary layer region to the blade trailing edge frequently leads to strong numerical oscillations. In the present work, two numerical algorithms for solving the compressible Navier-Stokes equations are considered. They are the modified implicit bidiagonal predictor-corrector scheme by MacCormack,[5] and the approximate factorization (AF) central differenced method by Beam and Warming[6] and Steger[7]. Since it is a well-tested numerical method, the AF scheme was used for validating the modified MacCormack scheme. The initial numerical stability problems were avoided by the use of the spectral radius formulation.[8] The full implicit MacCormack scheme (FIMC) is given as follows.

Predictor step:

$$\hat{u}^{\overline{n+1}} \equiv \hat{u}^n + C_1 \cdot \Delta\hat{u}^n + C_2 \cdot \delta\hat{u}^{\overline{n+1}}$$

with

$$[I - \Delta t\Delta^+ \mid \hat{A} \mid {}^n_{ij}][I - \Delta t\Delta^+ \mid \hat{B} \mid {}^n_{ij}]C_2\delta u^{n+1}_{ij} = C_2\Delta\hat{u}^n_{ij} \tag{1}$$

Corrector step:

$$\hat{u}^{n+1} = \tfrac{1}{2}[\hat{u}^n + \hat{u}^{\overline{n+1}} + C_1\Delta\hat{u}^{\overline{n+1}} + C_2\delta\hat{u}^{n+1}]$$

with

$$[I + \Delta t\Delta^- \mid \hat{A} \mid {}^{\overline{n+1}}_{ij}][I + \Delta t\Delta^- \mid \hat{B} \mid {}^{\overline{n+1}}_{ij}]C_2\delta u^{n+1}_{ij} = C_2\Delta\hat{u}^{\overline{n+1}}_{ij} \tag{2}$$

In the above, C_1 and C_2 are constants based on the local Courant-Friedrichs-Lewy (CFL) number and $|\hat{A}|$ and $|\hat{B}|$ are 4×4 matrices derived from the Euler flux Jacobians with viscous terms added to the diagonal elements. In order to improve the efficiency of this algorithm, the $|\hat{A}|$ and $|\hat{B}|$ in the implicit step are substituted by their special radii, $\lambda_{A,SR}$ and $\lambda_{B,SR}$. For example, the spectral normal of the flux Jacobian $|\hat{A}|$ is

$$\lambda_{A,SR} = |U_\xi| + C\sqrt{\xi_x^2 + \xi_y^2} + \frac{2\nu}{\rho}\left(\xi_x^2 + \xi_y^2\right) - \frac{1}{2\Delta t} \tag{3}$$

The resulting scheme is called spectral radius implicit MacCormack (SIMC). This procedure requires only the inversion of scalar bidiagonal matrices. Temporal accuracy of the solution is lost, but the scheme becomes less susceptible to oscillations at discontinuities. As it turns out, steady state accuracy is also compromised. This is due to the fact that the residual $\delta\hat{u}$ stays at relatively high values after decreasing by three orders of magnitude, especially in viscosity dominated regions where the largest eigenvalues of $|\hat{A}|$ and $|\hat{B}|$ are not dominant.

The SIMC scheme is ideally suited as an efficient scheme to obtain approximate viscous solutions. To enhance the steady-state accuracy, the full schemes are subsequently employed for a relatively small number of iterations. In the present analysis, several cases of internal flow geometries were studied. In each case, the SIMC was used as a preprocessor. Comparisons of convergence times are presented and are given in Ref. 9. Some comparisons with the inviscid results (wherever available) are also given and have demonstrated the importance of including the viscous terms in transonic cascade analysis.

Results

Initially, simpler geometries were selected to validate the codes and compare computation times, convergence rates, and quality of results. The results for the case of a supersonic nozzle and a diffusor with oblique shock have been previously reported.[8] Results of further flow predictions done for complex geometries are presented here (additional details are found in Ref. 10).

The flow past a wedge enclosed in a two-dimensional tunnel section is an internal flow configuration involving shocks and expansion waves and their interaction with the boundary layer. The geometry corresponds to the experimental arrangement reported in Ref. 11, which also contains the results of computations using the Euler equations. The wedge semi-angle is 9 deg, and the inflow Mach number is 1.45. The flow undergoes an oblique shock at the wedge and an expansion at the tunnel wall. Further downstream, the tunnel wall produces

Presented as Paper 85-0007 at the AIAA 23rd Aerospace Sciences Meeting, Reno, NV, Jan. 14–17, 1985; received Oct. 15, 1985; revision received April 23, 1986. Copyright © American Institute of Aeronautics and Astronautics, Inc., 1985. All rights reserved.

*Graduate Research Assistant; presently Research Engineer, Vigyan Research Associates Inc., Hampton, VA. Member AIAA.

†Assistant Professor, Aerospace Engineering Department; presently Associate Professor, Old Dominion University, Norfolk, VA. Member AIAA.

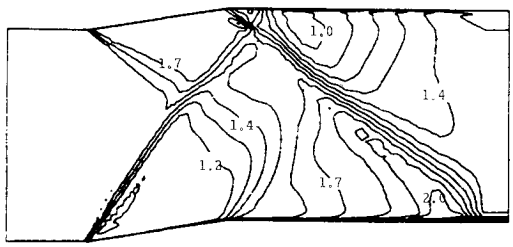

Fig. 1a Wedge flow: SIMC results after 500 steps.

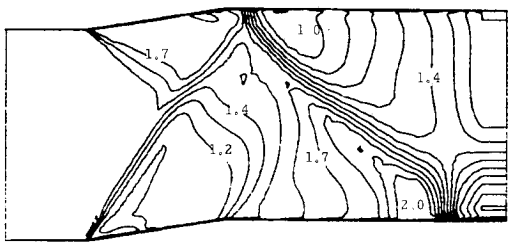

Fig. 1b Wedge flow: FIMC results after 500 steps from SIMC results.

a shock that interacts with expansion waves from the wedge. The dimensions of the geometry are such that the flow is expected to remain laminar throughout the test section. The grid near the wall has 12 to 15 points within a $y+$ value of 60, distributed exponentially with $y^+_{\min} = 2$.

Figure la shows the Mach number contour plots at the end of 500 iterations (CFL number of 25), using the simplified SIMC scheme. Comparison with results from Ref. 11 shows that the flow features are fairly well reproduced. The interaction of the shock with the expansion waves and its reflection from the tunnel wall can be distinguished. Figure 1b shows the results obtained after the application of the FIMC scheme for 500 iterations, starting with the SIMC results as the initial profile. Comparison with Fig. 1a shows that the two results are very close.

The important observation here is that the SIMC scheme works well as a rapid means of generating approximate solutions. The full algorithms could be subsequently used to improve the accuracy in substantially smaller numbers of iteration steps. The SIMC scheme was also found to be more robust compared to the full schemes. Generally, it could be run at higher CFL numbers and is tolerant of inaccurate initial distributions.

Several compressor cascade configurations were analyzed using the three numerical schemes. The results presented here are for a typical case that highlights the main conclusions in Ref. 11. The configuration is that of transonic flow in a multiple circular arc cascade for which inviscid numerical solutions have been obtained by Tong and Thompkins.[1] The relative inflow Mach number is 1.52, and the inflow direction is at an angle of 67.9 deg relative to the axis and is aligned with the blade suction surface slope at the leading edge. The static pressure rise ratio is 2·25. According to the transition criterion used in the present work, the transition from laminar to turbulent boundary layer is assumed at a point where $\mu_t > 14\mu_l$.

In the numerical sense, the flow in this case is more demanding than those considered previously. A strong passage shock is present in the blade region and the outflow is subsonic. The shock on the suction side is located close to the trailing edge. This, combined with the severe gradients in the near-wake region, produces numerical stability problems. To gain control of these problems, the SIMC scheme was applied for the first 500 iterations. The FIMC or AF scheme was subsequently used to refine the solution. Explicit and implicit damping terms were adjusted to reduce oscillations near the trailing edge.

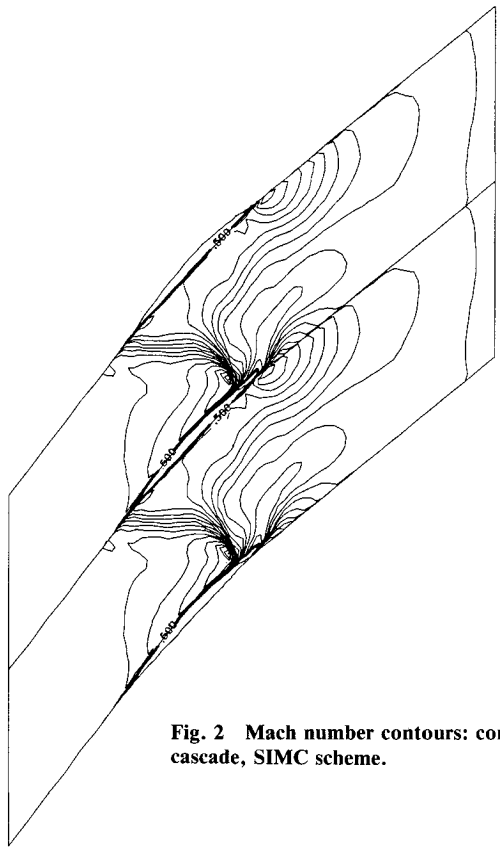

Fig. 2 Mach number contours: compressor cascade, SIMC scheme.

Figure 2 shows a plot of the Mach number contours at the end of only 500 iterations of the simplified SIMC scheme at a maximum CFL number of 150. It can be seen that the main features of the flow have been developed. A plot of the skin friction coefficient (not shown) showed mild separation at the suction side trailing edge.

The AF and FIMC schemes were applied, with the SIMC results as the starting profile. Convergence was obtained after 750 iterations at a maximum CFL number of 50. The results obtained from the FIMC scheme are nearly identical to the AF results. The pressure contours clearly show the leading edge shock and a subsequent milder passage shock interacting with each other in the region of the trailing edge. The Mach number contours show the strong viscous-inviscid interaction in this region. As a result, strong separation exists in the suction side trailing edge starting from about 75% chord.

For nearly identical conditions, it is interesting to compare these results with those of inviscid computation from Ref. 1. On the suction side, the pressure variation is very similar until about 60% chord. At this point, further expansion is prevented by the lambda shock. On the pressure side, the oblique shock in the viscous results turns the flow sufficiently so as to delay the pressure rise to some extent. It is thus obvious that the viscous effects play an important role in compressor transonic flow. Similar comparisons for other compressor geometries[9] have also substantiated the above observation.

Conclusion

Results have been presented for the solution of the full Navier-Stokes equations applied to predict viscous transonic flows in internal geometries using three numerical schemes. When compared with the inviscid Euler equation solution, the results showed marked variations in blade pressure and wake velocity field; it is therefore considered that Euler solvers applied to highly loaded transonic compressor cascades seem to be a questionable flow analysis tool. It has also been demonstrated that the simplified scheme employing spectral norms in

the implicit step is an efficient and rapid way of obtaining reasonably accurate solutions.

References

[1]Tong, S. S. and Thompkins, W. T., "A Design Calculation Procedure for Shock-Free or Strong Passage Shock Turbomachinery Cascades," *Journal of Engineering for Power*, Vol. 105, No. 2, April 1983, pp. 369–376.

[2]Thompkins, W. T., Tong, S. S., Bush, R. H., Usab, W. J., and Norton, R. J. G., "Simulations of Flow in Turbomachinery Cascades," AIAA Paper 83-0257, Jan. 1983.

[3]Thompkins, W. T. and Tong, S. S., "Inverse or Design Calculations for Non-Potential Flow in Turbomachinery Blade Passages," ASME Paper 81-GT-78, 1981.

[4]Steger, J. L., Pulliam, T. H., and Chima, R. V., "An Implicit Finite Difference Code for Inviscid and Viscous Cascade Flow," AIAA Paper 80-1427, July 1980.

[5]Kordulla, W. and MacCormack, R. W., "Transonic Flow Computation Using an Explicit-Implicit Method," *Proceedings of the Eighth International Conference on Numerical Methods in Fluid Dynamics*, Springer-Verlag, Berlin, 1982, pp. 286–295.

[6]Beam, R. and Warming, R. F., "An Implicit Factored Scheme for the Compressible Navier-Stokes Equation," AIAA Paper 77-645, June 1977.

[7]Steger, J. L., "Implicit Finite Difference Simulation of Flow About Arbitrary Two Dimensional Geometries," *AIAA Journal*, Vol. 16, July 1978, pp. 679-686.

[8]von Lavante, E. and Iyer, V., "Simplified Implicit Block-Bidiagonal Finite Difference Method for Soving the Navier-Stokes Equations," *AIAA Journal*, Vol. 23, July 1985, pp. 1130–1132.

[9]Iyer, V., "Numerical Solutions of Compressible Viscous Flow in Transonic Compressor Cascades," Ph.D. Dissertation, Dept. of Aerospace Engineering, Texas A&M University, College Station, May 1985.

[10]Iyer, V. and von Lavante, E., "Numerical Solutions of Viscous Transonic Flow in Turbomachinery Cascades," AIAA Paper 85-0007, Jan. 1985.

[11]Bryanston-Cross, P. J. and Denton, J. D., "Comparison of Interferometric Measurements and Computed Flow Around a Wedge Profile in the Transonic Region," ASME Paper 82-GT-258.

Optimal Barrel-Shaped Shells Under Buckling Constraints

J. Blachut*
University of Liverpool, Liverpool, England

I. Introduction

DOUBLY curved shells are common structural elements in various industries (aerospace, marine, civil engineering, etc.), and the buckling of such elements has received much attention in design.[1-6] It is generally agreed that the papers by McElman and Stein[1,2] sparked off detailed analysis of barreled shells. Their theory was limited to shallow shells and to buckling near the equator of a toroidal shell segment. Solutions were obtained, in a closed analytical form, for simply supported shells of both positive and negative curvature under internal or external pressure. A finite-element solution, as well as some experimental results presented in Ref. 7, did not completely agree with these first solutions.

The buckling and postbuckling behavior of axially compressed bowed-out and bowed-in shells was discussed in Ref. 8. Linear shell theory was used to find the buckling load, whereas the nonlinear theory was adopted to investigate the postbuckling state.

Qualitative ways of increasing the buckling resistance of barreled shells via meridional curvature change, stiffener eccentricity, and load eccentricity have been pointed out in Refs. 9–14. A substantial increase in the resistance of these shells to buckling has been observed, although these studies have not been based on optimal configurations.

The minimum weight of stiffened and barreled shells was examined in Ref. 15. In order to obtain the minimum weight configuration for a fixed axial load, the thickness of the skin and the thickness, depth, and spacing of solid rectangular stiffening rings and stringers were sought. Buckling was based on the linear membrane prebuckling state, and the gradient method with a penalty function was used.

The main aim of this paper is to establish, parametrically, the maximal compressive axial buckling load of a bowed-out shell. The wall thickness and the shell volume are kept constant. The buckling load increase is due to the change in the shell meridional curvature.

II. Formulation of Problem

Consider an elastic, clamped-clamped cylindrical shell of radius R_0, length L_0, constant thickness t, under axial compression F (see Fig. 1a). For a given volume of the cylindrical shell V_{cyl}, we seek the meridional radius of curvature r of the toroidal shell (see Fig. 1b) which possesses the same volume, thickness, boundary conditions, and truncation radius R_0, and also maximizes the buckling load.

III. Method of Solution

The volume of the toroidal shell (Fig. 1b) can be written as

$$V_{tor} = 4\pi(r^2 \sin\alpha - br\alpha)t \tag{1}$$

For a given value of the distance b, from the axis of revolution to the center of meridional curvature (see Fig. 1b), one can find the radius r from

$$V_{tor} = V_{cyl} \tag{2}$$

or

$$2(r^2 \sin\alpha - br\alpha) = R_0 L_0 \tag{3}$$

where R_0, L_0 are supposed to be given.

For a given value of the control parameter b we obtain, via Eq. (3), all the necessary geometrical parameters of the toroidal shell, which has the same volume as the original cylindrical shell. The computer code BOSOR 4[16] is used here to find the bifurcation buckling load and the collapse load. The latter is found by tracing out the load-displacement curve beyond the limit point (applying displacement-controlled analysis). Varying b in the range from zero to infinity, one obtains the truncated sphere and cylinder, respectively, as limiting cases.

IV. Numerical Results

Calculations were performed for L_0/R_0 varying from 0.25 to 4.0 and R_0/t varying from 100 to 1000. Figure 2 shows the change of bifurcation load as a function of curvature. For $L_0/R_0 = 4$, the optimal load is obtained for $R_0/(R_0+b) = 0.09$, regardless of the parameter R_0/t within the range of 100–1000. Analogous values for $L_0/R_0 = 2$ and $L_0/R_0 = 1$ are 0.17 and 0.28, respectively. Additional results for $L_0/R_0 = 0.5$ and $L_0/R_0 = 0.25$ are depicted in Fig. 3. It is seen that the optimal configurations do not depend on R_0/t for $0.5 \le L_0/R_0 \le 4.0$. However, for $L_0/R_0 = 0.25$ and $R_0/t < 300$, a change in meridional curvature no longer increases the buckling load. Axisymmetric collapse now be-

Received Jan. 15, 1986; revision received May 5, 1986. Copyright © American Institute of Aeronautics and Astronautics, Inc., 1986. All rights reserved.

*University Research Fellow, Department of Mechanical Engineering.